Available online at www.sciencedirect.com
SCIENCE DIRECT
Journal of Pharmaceutical and Biomedical Analysis 40 (2006) 1121–1130
JOURNAL OF PHARMACEUTICAL AND BIOMEDICAL ANALYSIS
www.elsevier.com/locate/jpba

Characterization of the cytochrome P450 enzymes and enzyme kinetic parameters for metabolism of BVT.2938 using different in vitro systems

Pawel Baranczewski *, Per Olof Edlund, Hans Postlind

Preclinical R&D, Biovitrum AB, Lindhagensgatan 133, SE-112 76 Stockholm, Sweden

Received 16 June 2005; received in revised form 7 September 2005; accepted 8 September 2005
Available online 22 November 2005

Abstract

An important step in the drug development process is identification of enzymes responsible for metabolism of drug candidates and determination of enzyme kinetic parameters. These data are used to increase understanding of the pharmacokinetics and possible metabolic-based drug interactions of drug candidates. The aim of the present study was to characterize the cytochrome P450 enzymes and enzyme kinetic parameters for metabolism of BVT.2938 [1-(3-{2-[(2-ethoxy-3-pyridinyl)oxy]ethoxy}-2-pyrazinyl)-2(*R*)-methylpiperazine], a potent and selective 5HT2c-receptor agonist. The enzyme kinetic parameters were determined for formation of three main metabolites of BVT.2938 using human liver microsomes and expressed cytochrome P450 (CYP) isoforms. The major metabolite was formed by hydroxylation of the pyridine ring (CL_{int} = 27 μl/mg min), and was catalysed by both CYP2D6*1 and CYP1A1, with K_m values corresponding to 1.4 and 2.7 μM, respectively. The results from enzyme kinetic studies were confirmed by incubation of BVT.2938 in the presence of the chemical inhibitor of CYP2D6*1, quinidine. Quinidine inhibited the formation of the major metabolite by approximately 90%. Additionally, studies with recombinant expressed CYP isoforms from rat indicated that formation of the major metabolite of BVT.2938 was catalysed by CYP2D2. This result was further confirmed by experiments with liver slices from different rat strains, where the formation of the metabolite correlated with phenotype of CYP2D2 isoform (Sprague–Dawley male, extensive; Dark Agouti male, intermediate; Dark Agouti female, poor metabolizer). The present study showed that the major metabolite of BVT.2938 is formed by hydroxylation of the pyridine ring and catalysed by CYP2D6*1. CYP1A1 is also involved in this reaction and its role in extra-hepatic metabolism of BVT.2938 might be significant.

Keywords: Drug metabolism; Enzyme kinetics; CYP2D6/CYP2D2; Dark Agouti rats

1. Introduction

BVT.2938 [1-(3-{2-[(2-ethoxy-3-pyridinyl)oxy]ethoxy}-2-pyrazinyl)-2(*R*)-methylpiperazine] is a potent and selective agonist of a 5HT2c receptor that has been demonstrated to reduce body weight in animal studies. Currently obesity is increasing health problem worldwide, with the prevalence of obesity 20.9% in the US population in 2001 [1]. BVT.2938 is recently examined for its preclinical properties and the present work describes the identification of the enzymes involved in metabolism of BVT.2938 and determination of the enzyme kinetic parameters.

Identification of the enzymes involved in the metabolism is one of the most important steps of drug metabolism studies during the drug discovery and development process.

The identification of enzymes involved in metabolism of drug candidate is useful for better understanding of genetic polymorphism in drug clearance and for prediction of potential metabolic-based drug–drug interactions [2–4].

Some drug metabolising enzymes, e.g. cytochrome P450 (CYP) 2D6 are polymorphic and their expression varies within a population [5,6]. When the drug candidate is metabolised via a polymorphic enzyme it might be very difficult to predict pharmacokinetic parameters for a whole populations and therefore, additionally studies using animal models or clinical studies are needed.

Currently, the risk for metabolic-based drug–drug interactions can be predicted early during the drug discovery process using in vitro approaches [4]. The enzyme affinity (K_i) of the drug candidate for different enzymes can be measured and compared to expected plasma concentration. If the ratio between the plasma concentration and K_i is equal to or above one, additional clinical studies are recommended

* Corresponding author. Tel.: +46 8 697 2423; fax: +46 8 697 3295.
E-mail address: pawel.baranczewski@biovitrum.com (P. Baranczewski).

0731-7085/$ – see front matter © 2005 Elsevier B.V. All rights reserved.
doi:10.1016/j.jpba.2005.09.006

to estimate the risk for metabolic-based drug–drug interactions [7].

The second important step of drug metabolism studies is the determination of enzyme kinetic parameters: K_m, V_{max} and CL_{int}. The determination of enzyme kinetic parameters for the metabolic reaction can be used for a better estimation of the drug candidate pharmacokinetics in human and to eliminate compounds with non-linear dose–exposure relationships [8]. The K_m value (Michaelis–Menten constant) is an indicator of the affinity between an enzyme and a substrate and it can also reflect at which concentration of the substrate, the enzymatic system will be saturated, with increasing risk at lower K_m values. Saturation of the enzymes may lead to non-linear kinetics of the drug candidate, which in turn may cause difficulties in prediction of dose and drug response [8,9]. Additionally, intrinsic clearance (the ratio V_{max}/K_m) can indicate the major metabolic pathway for elimination of the drug in human in vivo [8].

Previously, the identification of metabolites formed in incubations of BVT.2938 with human and animal liver microsomes as well as cryopreserved hepatocytes have been described [10]. In incubations with human liver microsomes eight metabolites were identified. Three of them: M2, hydroxylation of the pyridine ring; M7, *O*-deethylation of the pyridine ring; M8, *O*-dealkylation of the ethylene bridge, were formed at the highest rate. In the present studies different in vitro approaches like recombinant expressed enzymes, liver microsomes, tissue slices, and chemical inhibitors were used for further investigation into the metabolism of BVT.2938.

2. Materials and methods

2.1. Incubation of BVT.2938 with human and rat liver microsomes for determination of metabolic stability

Pooled human liver microsomes, rat Sprague–Dawley (SD) male and female liver microsomes were purchased from XenoTech LLC (Kansas City, KS, USA). The experiments for determination of metabolic stability were performed at 37 °C using 1 μM compound concentration, 1 mg/ml microsomal protein and 1 mM NADPH in a total volume of 150 μl of 100 mM phosphate buffer, pH 7.4. The incubation was started by the addition of NADPH (Merck, Darmstadt, Germany) and terminated with 75 μl of acetonitrile at 0, 2.5, 5, 10, 20 and 40 min. Precipitated proteins were removed by centrifugation at 3200 rpm for 15 min at 4 °C before analysis.

Concentrations of BVT.2938 were determined in supernatants using liquid chromatography–tandem mass spectrometry. After centrifugation, samples were injected without any further pre-treatment onto a Zorbax SB-C18 5 μm, 2.1 mm × 50 mm HPLC-column. The mobile phase consisted of 8 mM formic acid and acetonitrile and the column was eluted with a linear gradient from 5 to 95% acetonitrile at a flow rate of 0.3 ml/min. Detection was made using a Micromass Quattro II mass spectrometer operated in positive ion mode electrospray with multiple reaction monitoring. The transition monitored was m/z 360 [MH^+] → m/z 221. The incubations terminated prior to addition of NADPH were used as calibration standards, defined as 100%. Sample concentrations were calculated by comparing peak areas, and expressed as the fraction (in %) of remaining compound. The in vitro $t_{1/2}$ and intrinsic clearance of BVT.2938 in liver microsomes were calculated using the in vitro half-life method [11].

2.2. Incubation of BVT.2938 with human expressed CYP isoforms for determination of potential drug–drug interactions

BVT.2938 was dissolved in DMSO and added directly into incubations to a maximum final DMSO concentration of 1%. DMSO was added to control incubations (without BVT.2938). The inhibitor concentrations were between 0.1 and 100 μM in a total incubation volume of 100 μl with 25 or 100 mM KPO_4 buffer, pH 7.4. Incubations were performed in triplicates. The concentrations of marker substrates were at K_m and $3K_m$ for each different marker. The reaction was started by addition of NADPH to a concentration of 1 mM and terminated with 50 μl acetonitrile or 60% acetonitrile/40% 0.1 M Tris, pH 9.0.

The activity of CYP1A1 was estimated using [^{14}C]-chlorzoxazone as a marker substrate at a concentration of 9 μM. The marker substrate was incubated over 60 min at 37 °C in the presence of 2 pmol of CYP1A1, 1 mM NADPH and 1% of DMSO (control incubations) or BVT.2938 solution in DMSO. The incubations were analyzed on a pre-column (Opti-Guard C8, 2 μm, 3 mm) and a Zorbax SB C8 column (5 μm, 150 mm × 4.6 mm). The column was eluted using isocratic conditions, 35% A and 65% B (mobile phase A: 90% water, 10% methanol and 0.2% acetic acid; mobile phase B: 90% methanol, 10% water and 0.2% acetic acid) over 5 min, at a flow rate of 1.5 ml/min and a scintillation liquid flow of 4.5 ml/min.

CYP1A2 was measured using 3-cyano-7-ethoxycoumarin as marker substrate, at a concentration of 3.5 μM. Amount formed of 3-cyano-7-hydroxycoumarin was detected with a fluorescence method using an excitation wavelength of 405 nm and emission wavelength of 460 nm. The fluorescence was measured with a Victor 2, 1420 multilable counter instrument from Wallac (EG&G Wallac, Turku, Finland).

Inhibition of CYP2C9*1 (Arg144) was measured using [^{14}C]-diclofenac as a marker substrate at a concentration of 10 μM. HPLC analysis of marker substrate was performed using a pre-column (Opti-Guard C8, 2 μm, 3 mm) and a Zorbax SB C8 column (5 μm, 150 mm × 4.6 mm). The mobile phase consisted of A (90% H_2O/10% MeOH/0.2% acetic acid) and B (90% MeOH/10% H_2O/0.2% acetic acid). The column was eluted using stepwise gradient (0 min/0% B, 5 min/90% B, 10 min/90% B, 11 min/0% B), at a flow rate of 1.5 ml/min and a scintillation liquid flow of 4.5 ml/min.

Inhibition of CYP2D6*1 was measured using 5 μM [^{14}C]-dextromethorphan as marker substrate and 3 M Empore extraction plate ethyl (C2) to separate the metabolite dextrophan. The detection was made using a TopCount NXT.

Inhibition of CYP3A4 was measured using [^{14}C]-testosterone as marker substrate for formation of 6β-hydroxytestosterone determined by a HPLC system equiped with a pre-column (Newguard 7 μm RP 18, 3.2 mm × 15 mm)

and a Zorbax SB C18 column (5 μm, 150 mm × 4.6 mm). The mobile phase consisted of A (20% acetonitrile, 80% water and 0.25% acetic acid) and B (65% acetonitrile, 35% water and 0.25% acetic acid). The column was eluted using isocratic conditions, 30% of A and 70% of B over 5 min at a flow rate of 2.0 ml/min and a scintillation liquid flow of 6.0 ml/min.

2.3. Incubations of BVT.2938 with individual human and rat expressed CYP isoforms and FMOs

All recombinant expressed enzymes used in this study were purchased from BD Biosciences (Bedford, MA, USA). A 5 pmol of recombinant expressed human cytochrome P450 isozymes (CYPs: 1A1, 1A2, 1B1, 2A6, 2B6, 2C8, 2C9*1, 2C19, 2D6*1, 2E1, 3A4, 3A5 and 4A11), rat cytochrome P450 isozymes (CYPs: 1A1, 1A2, 2A2, 2B1, 2C6, 2C11, 2C12, 2C13, 2D1, 2D2, 3A1 and 3A2), or FMO1, or FMO3, or FMO5, or 10 μg of control microsomes per 100 μl were incubated in triplicates with 10 μM of [^{14}C]-BVT.2938, giving a final concentration of ethanol equal to 1%. The samples with isozymes CYP1A1, CYP1A2, CYP1B1, CYP2D6*1, CYP3A4, FMO1, FMO3, FMO5 and with control microsomes were incubated in 100 mM KPO_4, pH 7.4 buffer, while 50 mM was used for CYP2B6, CYP2C8 and CYP2E1 and incubations with CYP2C9*1 and CYP2C19 were performed with 25 mM KPO_4, pH 7.4 buffer. CYP2A6 was incubated in 50 mM Tris buffer, pH 7.4. The incubations were initiated by addition of NADPH (final concentration of 1 mM) and terminated after 60 min by addition of 50 μl of 3% trichloroacetic acid in buffer. Precipitated proteins were removed by centrifugation at 3200 rpm for 15 min at 4 °C and the supernatants were analyzed using HPLC/Radiomatic system.

2.4. Incubation of BVT.2938 with human liver microsomes for determination of enzyme kinetic parameters

Different concentrations of [^{14}C]-BVT.2938: 0.1, 0.25, 0.5, 0.75, 1, 2.5, 5, 7.5, 10, 25, 50, 75 and 100 μM were incubated in triplicates in the presence of 100 μg microsomal proteins in 100 mM KPO_4, pH 7.4, at 37 °C (final incubation volume of 100 μl). The samples were incubated in triplicates. The incubations were initiated by addition of NADPH (final concentration of 1 mM) and terminated after 15 min (the incubation time was chosen to be in the linear range) by addition of 50 μl of 3% trichloroacetic acid in 100 mM KPO_4, pH 7.4. Precipitated proteins were removed by centrifugation at 3200 rpm for 15 min at 4 °C and the supernatants were analyzed using HPLC/Radiomatic system.

*2.5. Incubations of BVT.2938 with human CYPs: 1A1, 2D6*1 and 3A4 for determination of enzyme kinetic parameters*

CYP1A1, or CYP2D6*1, or CYP3A4 were incubated in triplicates with [^{14}C]-BVT.2938 at concentrations 0.1, 0.25, 0.5, 0.75, 1, 2.5, 5, 7.5, 10, 25, 50, 75 and 100 μM. The activity of the enzyme was 0.03 pmol/μl, in a total incubation volume of 100 μl of 100 mM KPO_4, pH 7.4. The incubations were started by addition of NADPH (1 mM) and terminated after 10 min by addition of 50 μl of 3% trichloroacetic acid in 100 mM KPO_4, pH 7.4. Control incubations were performed in triplicates using 10 μg of microsomes from insect control cells containing no detectable activity of P450 enzymes and 1, 10 and 100 μM of [^{14}C]-BVT.2938. Precipitated proteins were removed by centrifugation at 3200 rpm for 15 min at 4 °C and the supernatants were analyzed using a HPLC/Radiomatic system.

2.6. Incubation of BVT.2938 with human liver microsomes and specific chemical inhibitors

[^{14}C]-BVT.2938 was incubated at a concentration of 5 μM in the presence of human liver microsomes and different CYP isozyme-specific inhibitors; CYP1A (α-naphthoflavone), CYP2C9 (sulfaphenazole), CYP2D6 (quinidine), CYP3A (ketoconazole). The inhibitors were dissolved in methanol and added to the incubations at a final concentrations of 1, 10 or 50 μM for all inhibitors except ketoconazole, where the final concentrations were 0.01, 0.1 or 1 μM. The amount of methanol was 1% in all incubations. Incubations were performed in triplicates for 15 min at 37 °C, using a final protein concentration of 1 mg/ml and an NADPH concentration of 1 mM. Total incubation volume was 100 μl (100 mM KPO_4 pH 7.4). The incubations were initiated by the addition of NADPH. Control incubations containing 1% solvent (methanol), without any inhibitor, were also performed. All reactions were terminated by the addition of 50 μl of 3% trichloroacetic acid in 100 mM KPO4, pH 7.4. Precipitated proteins were removed by centrifugation at 3200 rpm for 15 min at 4 °C and the supernatants were analyzed using a HPLC/Radiomatic system.

2.7. Incubation of BVT.2938 with rat liver slices

Liver from the following rat strains: Sprague–Dawley (SD) male, SD female, Dark Agouti (DA) male and DA female were used. All animals were 6–8 weeks old and weighed approximately 200 g. The livers were washed with ice-cold Krebs–Henseleit buffer and tissue cores of 8 mm diameter were prepared using a motor-driven corning tool from Vitron, Inc. (Tuscon, AZ, USA). The best cores were used for slice preparation. Liver slicing was performed in ice-cold Krebs–Henseleit buffer using Brendel/Vitron tissue slicer from Vitron, Inc. The slicing buffer was gassed before and during slicing with carbogen (95% O_2/5% CO_2). Slices diameter was 8 mm and weight 25–30 mg. Fresh cut slices were placed in a six-well plate: one slice per well with 1.5 ml of incubation medium—Williams's medium E with Glutamax-I. BVT.2938 was dissolved in DMSO and added directly to the incubation to a final concentration of 5 μM. [^{14}C]-BVT.2938 was dissolved in methanol and added directly to the incubation to a final concentration of 5 μM. In addition differences in CYP2D2 activity was analyzed by incubating liver slices from every rat strain with propranolol, at a final concentration of 10 μM. The final concentration of DMSO and methanol was less than 0.2% (v/v). The same amounts of DMSO and methanol were added to control incubations

without BVT.2938 or propranolol. The slices were incubated for 4 and 8 h at 37 °C, under continuous carbogen (95% O_2/5% CO_2) flow. After incubation the slices were transferred to tubes and homogenized for 30 s using a Ultra-Turrax. Ice-cold acetonitrile (1.5 ml) was added to terminate the reaction and precipitated proteins were removed by centrifugation at 3500 rpm for 15 min at 4 °C. The acetonitrile was evaporated under nitrogen and samples were filtered through 0.45 μm micro-spin cellulose filters from Alltech Assoc., Inc. (IL, USA).

2.8. HPLC/Radiomatic conditions for analysis of samples from the incubations

The parent compound ([^{14}C]-BVT.2938) remaining and metabolites formed, were analyzed using Hewlett-Packard 1100 HPLC system connected to a flow scintillation detector, Packard Radiomatic 500TR series. The samples were analyzed using a Phenomenex column: Luna C18 (2), 4.6 mm × 150 mm with 5 μ particles. Mobil phase A: 2% methanol, 0.02% TFA; mobile phase B: 100% methanol, 0.02% TFA; gradient from 25% to 45% of B over 34 min at a flow rate 1 ml/min with a scintillation liquid flow of 3 ml/min (Ultima FLO-AP).

2.9. Calculations

Maximal velocity (V_{max}), Michaelis–Menten constant (K_m) and intrinsic clearance (CL_{int}) as well as IC_{50} and K_i values were calculated using non-linear regression by the GraphPad PRISM™ software, version 2.0 (GraphPad Software, Inc., San Diego, CA, USA). Michaelis–Menten, Lineweaver–Burk and Eadie–Hofstee plots were plotted.

3. Results

The intrinsic clearance of BVT.2938 after incubation with human and rat SD male and female liver microsomes was the highest for male rat and the lowest for the samples incubated with human microsomes (Table 1).

BVT.2938 is metabolized into several metabolites in the presence of human liver microsomes and human cryopreserved hepatocytes [10]. Three of them: M2, hydroxylation of the pyridine ring; M7, *O*-deethylation of the pyridine ring; M8, *O*-dealkylation of the ethylene bridge, were formed at the highest rate (Fig. 1). Additionally, the experiments with recombinant expressed human CYP isozymes showed that two isoforms, namely CYP1A1 and CYP2D6*1 were involved in the formation of M2 and M7 metabolite (Fig. 2). Therefore, the enzyme kinetic parameters for metabolism of BVT.2938 into these major metabolites were determined by measuring the consumption of BVT.2938 and formation of M2, M7 and M8 metabolites at substrate concentrations from 0.1 to 100 μM in the presence of human liver microsomes as well as human expressed enzymes.

Under the conditions used, the conversion of BVT.2938 into the M2 metabolite using Michaelis–Menten plot had a K_m equal to 5.5 μM (Fig. 3A and Table 2). However, using the Lineweaver–Burk plot the K_m value obtained for the formation of M2 was 2.0 μM (Fig. 3B and Table 2). The results obtained from the Eadie–Hofstee plot indicated that formation of the M2 metabolite was catalyzed by two enzymes (Fig. 3C). The K_m value for the first enzyme was 2.0 μM and for the second enzyme 5.0 μM respectively (Table 2). In experiments with human recombinant expressed CYPs, CYP2D6*1 was found to have a K_m of 1.4 μM, and CYP1A1 a K_m of 2.6 μM. Summary of the enzyme kinetic results for the formation of the M2 metabolite after incubation of BVT.2938 with human liver microsomes and these CYP isoforms are presented in Table 2.

The results from Michaelis–Menten, Lineweaver–Burk and Eadie–Hofstee plots for the formation of M7 in the presence of human liver microsomes are shown in Table 3. The Eadie–Hofstee plot suggested that two enzymes also were involved in the formation of M7 metabolites: one having a K_m equal to 0.8 μM and the second enzyme with a K_m of 7.8 μM (Fig. 4). Experiments using human expressed CYP isozymes indicated that both CYP1A1 and CYP2D6*1 were able to catalyze the formation of M7—CYP2D6*1 was determined to have a K_m value equal to 1.0 μM, and CYP1A1 a K_m equal to 3.8 μM (Table 3).

The Eadie–Hofstee plot indicated that more than one enzyme was involved in the formation of the M8 metabolite in incubation with human liver microsomes: enzyme 1 with K_m and V_{max} equal to 26 μM and 248 pmol/mg min, and enzyme 2 with K_m and V_{max} equal to 6.1 μM and 131 pmol/mg min, respectively. The results obtained with the

Table 1
Summary of metabolic stability data for BVT.2938 in incubations with human and rat SD male and female liver microsomes

Liver microsomes	In vitro $t_{1/2}$ (min)	In vitro CL_{int} (μl/mg min)	In vitro CL_{int} (ml/kg BW min)
Human (pool)	9.2	75	75
Rat SD male	2.6	270	594
Rat SD female	4.2	165	363

CL_{int}: intrinsic clearance.

Table 2
Summary of the enzyme kinetics for formation of the M2 metabolite after incubation of BVT.2938 with human liver microsomes, CYP2D6*1 and CYP1A1

Plot	K_m (μM)	V_{max} (pmol/mg min)	CL_{int} in vitro (μl/mg min)
Human liver microsomes			
Michaelis–Menten	5.5	106	19
Lineweaver–Burk	2.0	68	34
Eadie–Hofstee (enzyme 1)	2.0	67	34
Eadie–Hofstee (enzyme 2)	5.0	109	22
CYP2D6*1			
Michaelis–Menten	1.2	716	597
Lineweaver–Burk	1.5	716	477
Eadie–Hofstee	1.6	750	469
CYP1A1			
Michaelis–Menten	2.0	80	40
Lineweaver–Burk	3.1	79	25
Eadie–Hofstee	2.9	86	30

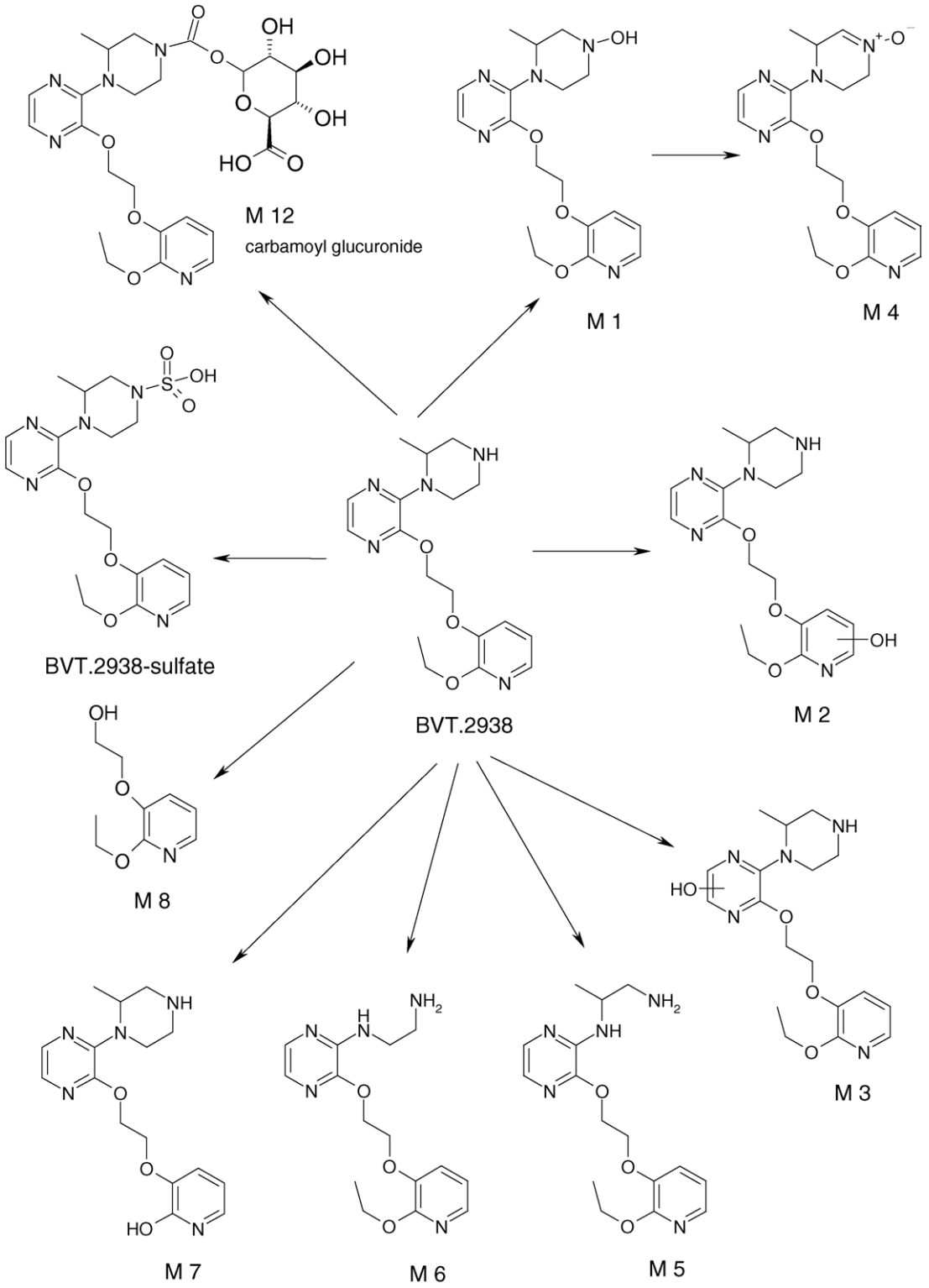

Fig. 1. Chemical structure of BVT.2938 and its metabolites formed after in vitro incubation with human liver microsomes and rat liver slices.

Michaelis–Menten plot confirmed the parameters for the first, low affinity enzyme (K_m = 25 μM and V_{max} = 256 pmol/mg min, CL_{int} = 10 μl/mg min), and the Lineweaver–Burk plot results for the second, high affinity enzyme (K_m = 7.4 μM and V_{max} = 108 pmol/mg min, CL_{int} = 15 μl/mg min). Experiments using human expressed CYP isozymes indicated that three enzymes were able to form the M8 metabolite, namely CYP2D6*1, CYP3A4 and to low extent CYP1A1. The results obtained with incubations of BVT.2938 and CYP3A4 indicated that CYP3A4 was the major isoform responsible for formation of M8 metabolite (K_m = 7.3 μM, V_{max} = 390 pmol/mg min and CL_{int} = 53 μl/mg min).

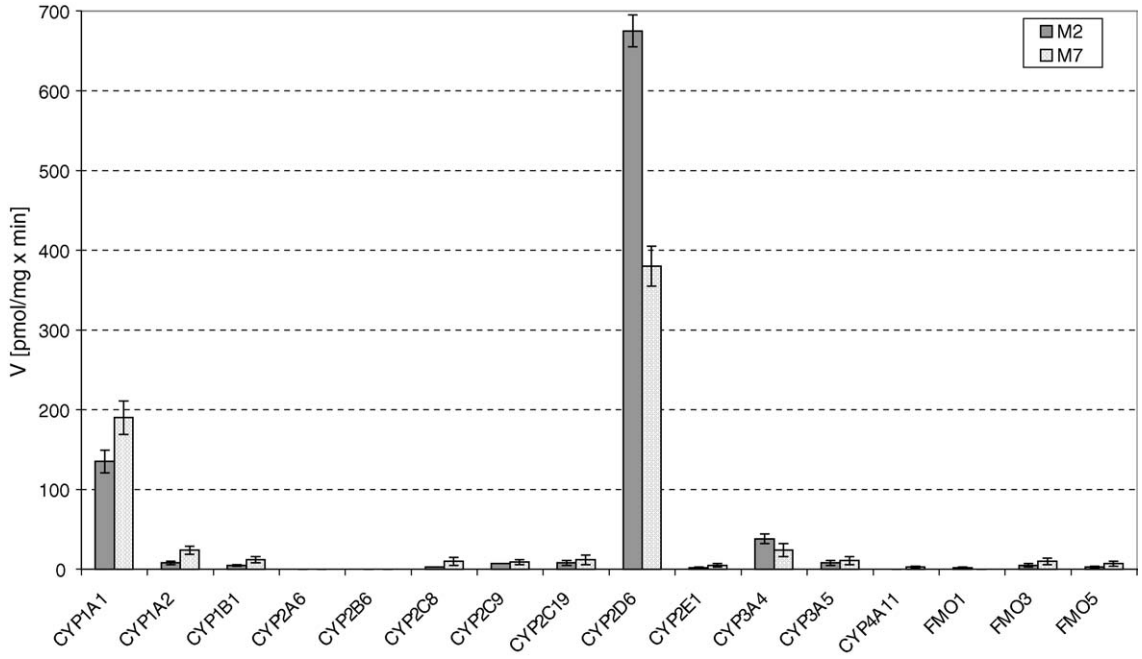

Fig. 2. Formation of M2 and M7 metabolites after incubation of 10 μM BVT.2938 with different CYP isozymes and FMOs.

The enzyme kinetic results for two major metabolites of BVT.2938—M2 and M7, were confirmed in experiments with chemical inhibitors of CYP2D6 (quinidine), CYP1A1 (α-naphthoflavone), CYP2C9 (sulfaphenazole) and CYP3A4 (ketoconazole). Quinidine inhibited formation of M2 and M7 metabolites by 90 and 95%, respectively, and α-naphthoflavone by approximately 40 and 30%, respectively (Fig. 5). Ketoconazole at the final concentration of 0.01 μM was responsible for approximately 20% of inhibition of the formation of both metabolites. However, no further inhibition was observed with increased concentration of ketoconazole up to 1 μM (Fig. 5). Sulfaphenazole did not have any significant influence on the formation of M2 and M7.

Table 3
Summary of the enzyme kinetics for the formation of M7 metabolite after incubation of BVT.2938 with human liver microsomes, CYP2D6*1 and CYP1A1

Plot	K_m (μM)	V_{max} (pmol/mg min)	CL_{int} in vitro (μl/mg min)
Human liver microsomes			
Michaelis–Menten	5.5	53	9.6
Lineweaver–Burk	1.3	33	27
Eadie–Hofstee (enzyme 1)	0.8	27	33
Eadie–Hofstee (enzyme 2)	7.8	68	8.7
CYP2D6*1			
Michaelis–Menten	1.0	343	343
Lineweaver–Burk	0.9	331	368
Eadie–Hofstee	1.0	356	356
CYP1A1			
Michaelis–Menten	3.7	227	61
Lineweaver–Burk	3.2	214	67
Eadie–Hofstee	4.5	268	60

Five other metabolites of BVT.2938 were formed at lower concentrations with human liver microsomes. Due to the low concentrations no enzyme kinetic parameters were investigated for these metabolites. However, human expressed CYP isoforms and FMOs were used to determine which enzymes that were involved in formation of these metabolites. *N*-hydroxylation at the piperazine ring of BVT.2938 (M1 metabolite) was only catalysed by FMO1. CYP3A4 and to lower extent CYPs: 2D6*1 and 1A1 were involved in formation of the following metabolites: M3, hydroxylation at the pyrazine ring, M5 and M6, piperazine ring opening (Fig. 1).

The enzyme kinetic studies were confirmed in experiments for prediction of potential drug–drug interactions for BVT.2938. The highest risk for metabolic-based drug–drug interactions was estimated for CYP1A1 with K_i value of 1.0 μM (Table 4). Additionally, BVT.2938 was showed to be a competitive inhibitor of CYP2D6*1 (K_i = 3.4 μM) and CYP3A4 (K_i = 10 μM). The lowest risk for interactions were predicted between BVT.2938 and compounds/drugs metabolized by CYP1A2 and CYP2C9*1 (Arg144) (Table 4).

The previous study showed that BVT.2938 was metabolised to the same metabolites in rat and human microsomes [10]. In order to characterize the rat CYPs responsible for metabolism of BVT.2938, the compound was incubated with 12 different rats recombinant expressed CYPs. Under these conditions, the major CYP involved in formation of M2 metabolite was CYP2D2 with an activity of 67 pmol/mg min. Two more rat CYPs also catalysed the formation of M2, CYP1A1 and CYP2C6, at an activity of 30 and 13 pmol/mg min, respectively. The formation of M7 metabolite was catalysed by the following rat CYPs: 2D2, 1A1 and 2C6, at 166, 83 and 20 pmol/mg min, respectively. The M1 metabolite was formed in incubations with CYP2C11 with an activity of 17 pmol/mg min, and formation of two metabolites

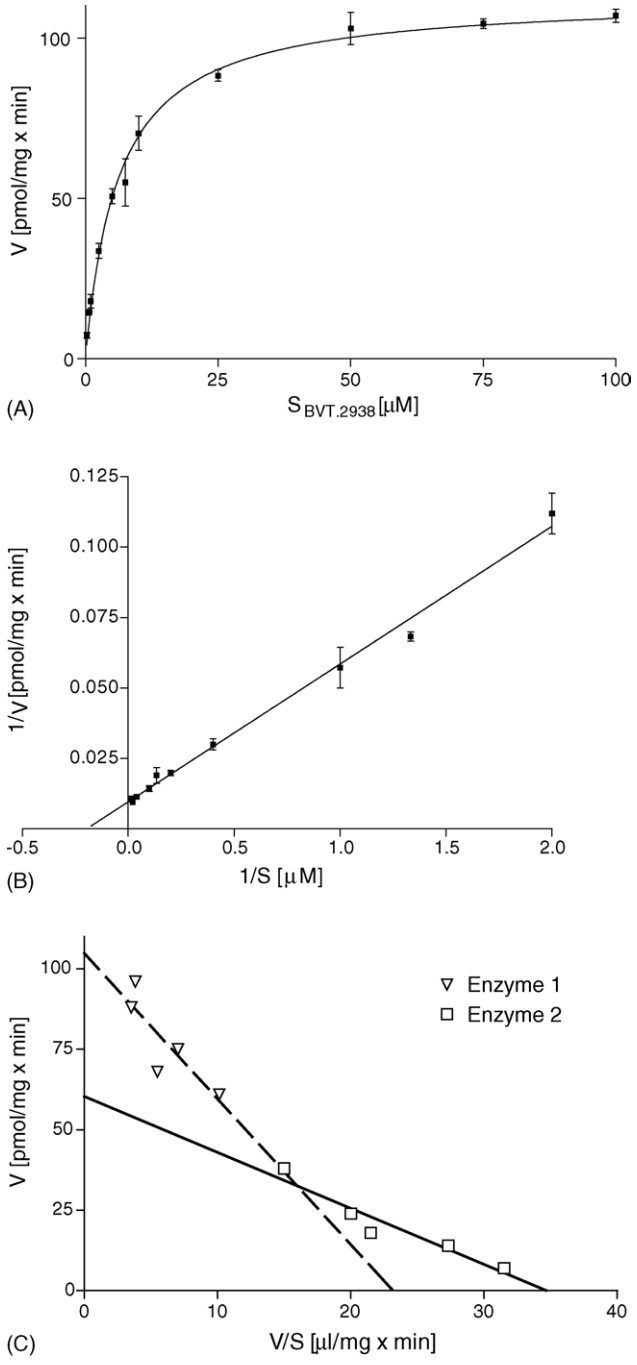

Fig. 3. The representative plots for formation of M2 metabolite after incubation of BVT.2938 with human liver microsomes. (A) Michaelis–Menten plot, (B) Lineweaver–Burk plot and (C) Eadie–Hofstee plot.

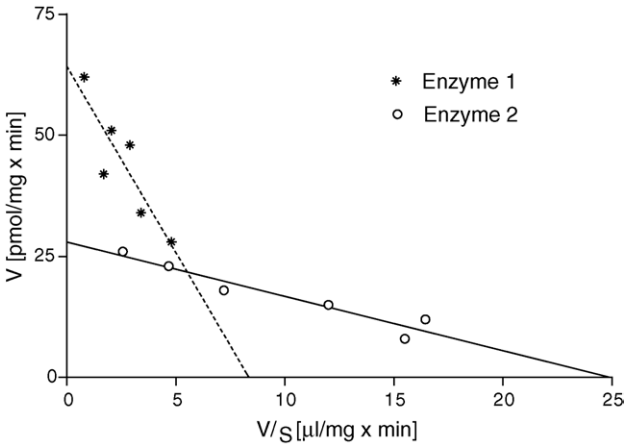

Fig. 4. The Eadie–Hofstee plot for formation of M7 metabolite after incubation of BVT.2938 in the presence of human liver microsomes.

related to piperazine ring opening, M5 and M6, was catalysed by CYPs: 3A1 and 3A2 as well as CYP1A1 and CYP2C6 with low activity.

The influence of CYP2D2 isoform on metabolism of BVT.2938 was further investigated using liver slices from different rat strains. The metabolite pattern obtained for BVT.2938 was the same after incubation with rat liver slices as compared to microsomes, except that direct conjugations of BVT.2938 with sulfuric and glucuronic acid (via carbamate) were also identified (Fig. 1). However, the level of the metabolites differed between tested rat strains after 8 h of incubation (Fig. 6). The experiments showed that the formation of metabolites related to CYP2D2 activity, namely M2 and M7 metabolites, decreased in the following order: SD male, DA male and DA female liver slices. No significant differences were detected in formation of the metabolites between SD male and female rat liver slices (Fig. 6). BVT.2938 remaining and BVT.2938-sulfate showed opposite upward trend, the lowest level was detected with liver slices from SD male rat, higher with DA male and the highest with DA female rat liver slices. The same trend regarding the formation of metabolites of BVT.2938 with liver slices from different rat strains was also observed after 4 h of incubation (data not shown).

Liver slices from different rat strains were also incubated with propranolol, and formation of 7-hydroxylated metabolite was determined. The highest turnover of propranolol to 7-hydroxylated metabolite was detected in incubations with SD male and female liver slices with an activity

Table 4
Summary of the data obtained after incubation of BVT.2938 with human expressed CYP isoforms for determination of drug–drug interactions

Enzyme	Percent of inhibition (%)			IC_{50} (μM)	K_i (μM)	Type of inhibition
	1 μM	10 μM	100 μM			
CYP1A1	43	87	96	2.0	1.0	Competitive
CYP1A2	0	12	72	ND	ND	ND
CYP2C9*1	0	17	81	ND	ND	ND
CYP2D6*1	20	62	86	6.8	3.4	Competitive
CYP3A4	6	43	94	20	10	Competitive

ND: not determined.

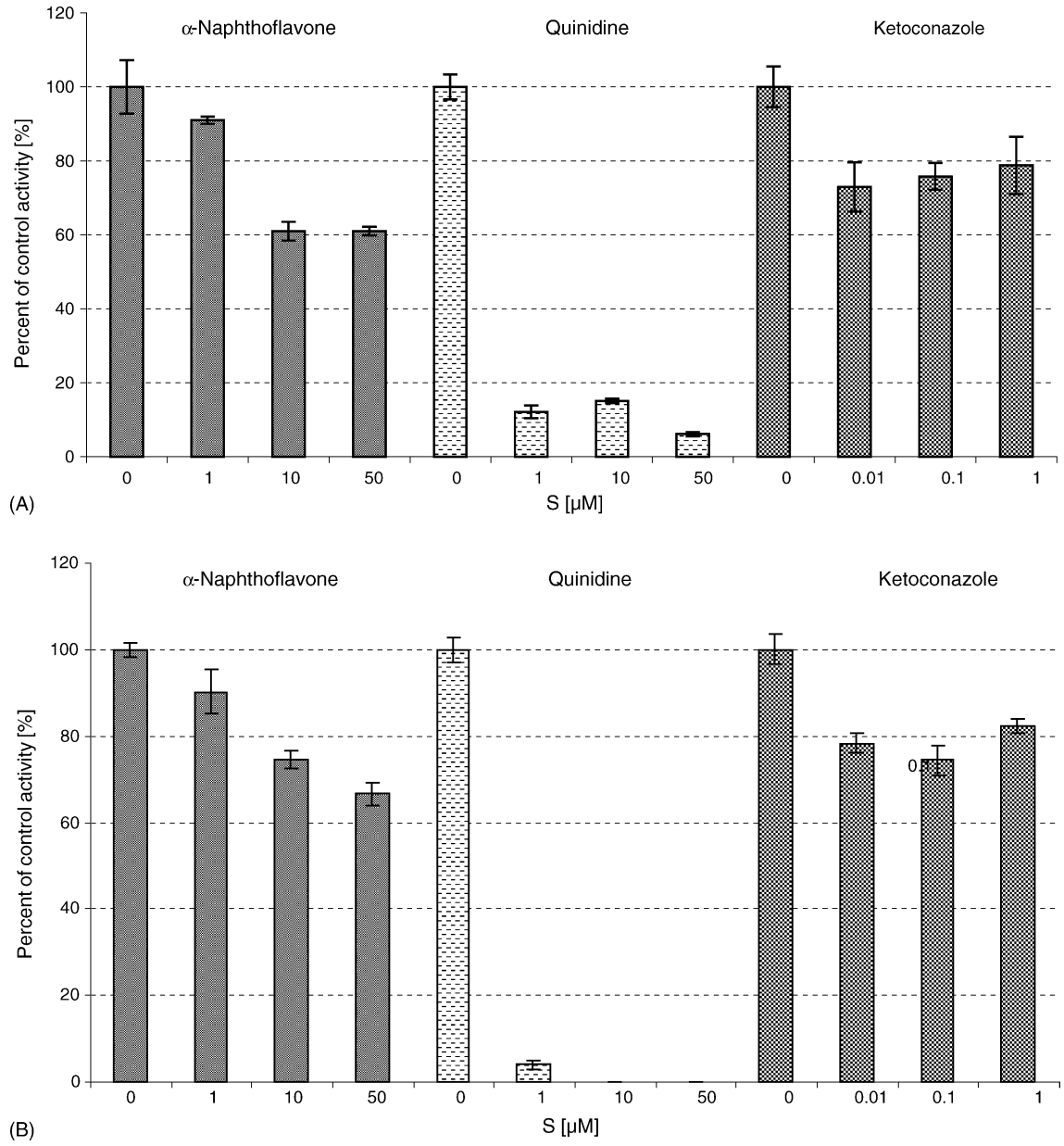

Fig. 5. Effect of cytochrome P450 specific, chemical inhibitors: α-naphthoflavone, quinidine and ketoconazole on the formation of M2 (A) and M7 (B) metabolites after incubation of 5 μM [^{14}C]-BVT.2938 with human liver microsomes. All values are mean values from duplicates and the standard deviation is calculated from duplicates.

of 23 and 21 pmol/mg min, respectively. Lower formation of 7-hydroxypropranolol was obtained in DA male rat slices (9 pmol/mg min) and the lowest in incubation with DA female liver slices (2 pmol/mg min).

4. Discussion

The human and animal liver fractions and recombinant expressed metabolising enzymes offer new possibilities for identification of the enzymes involved in metabolic reactions and for kinetic characterization of the reactions [7,12]. This study demonstrates an example how these models can be used to characterize a drug candidate at an early stage in drug discovery and development. Analysis of the metabolic stability performed at an early discovery stage showed that the compound might be metabolised to a high extent by CYPs. Data from the CYP inhibition screen were used for prediction of possible interactions between BVT.2938 and drugs, which already are present on the market for treatment of obesity. Two CYP isoforms: 3A4 and 2C9 are involved in metabolism of a lipase inhibitor, Xenical [13,14]. Based on the results of the present studies it might be concluded that low risk for drug–drug interactions exist between BVT.2938 and Xenical. Another anti obesity drug present on the market is Meridia [14]. Unfortunately, no information regarding the metabolism of this drug or several other compounds which are under development for treatment of obesity, are available at present. The competitive type of inhibition between BVT.2938 and CYPs suggested that these isoforms might also

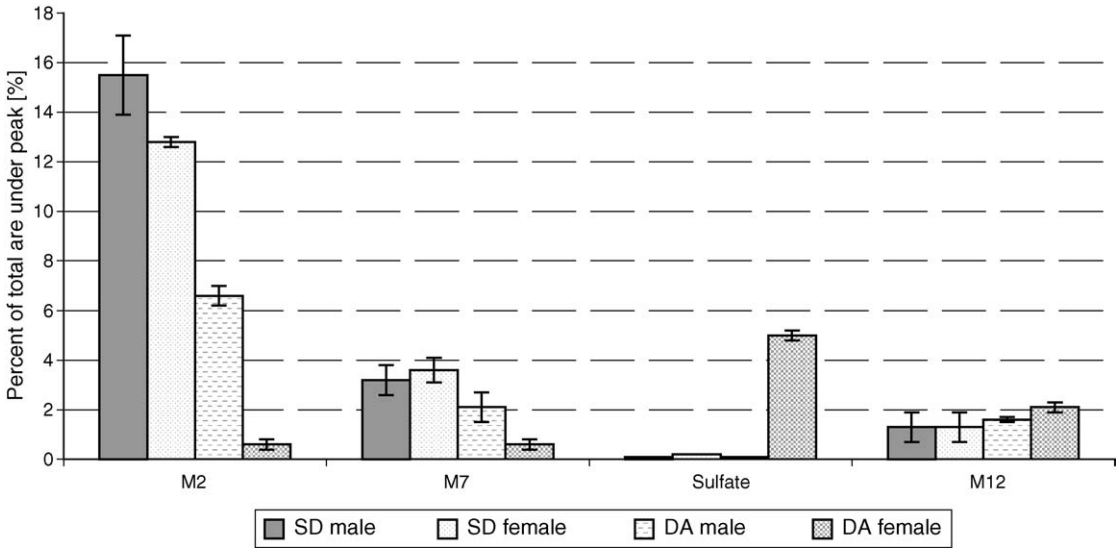

Fig. 6. Percent of total peak area for M2, M7, sulfate and carbamoyl glucuronide of BVT.2938 after 8 h incubations with rat liver slices from different rat strains: SD male, SD female, DA male and DA female. All values are mean values from duplicates and the standard deviation is calculated from duplicates.

be involved in the metabolism of BVT.2938. Therefore, further in vitro studies for identification and kinetic characterization of the metabolic enzymes involved in the metabolism of BVT.2938 were initiated. The hepatic CYP isoforms responsible for the formation of the major metabolite of BVT.2938 were CYP2D6*1 and CYP2D2 in incubations with human and rat recombinant expressed CYPs, respectively. Because CYP2D6 is one of the polymorphic isoforms of CYP [5], further studies with liver slices from different rat strains were performed. Three rat strains with different CYP2D2 phenotype were selected: SD male and female, extensive metabolizer; DA male, intermediate; DA female, poor metabolizer of CYP2D2 [15–17]. The differences in activity of CYP2D2 across rat strains were confirmed using a specific reaction for CYP2D2: propranolol 7-hydroxylation [18]. The results obtained confirmed the importance of CYP2D2 activity for the metabolism of BVT.2938, and changes in activity of the isoform influenced the total metabolism of the compound. Surprisingly, the lower formation of the major metabolites of BVT.2938 related to decrease of CYP2D2 activity resulted not only in decreased of consumption of the parent compound but also in an increase in the formation of the sulfate metabolite of BVT.2938. This metabolite was formed by direct conjugation of BVT.2938 and could be detected only in incubations with hepatocytes or liver slices [10]. This observation suggested that further studies on BVT.2938 metabolism by CYP2D6 should include human hepatocytes and/or tissue slices.

The second important CYP isoform responsible for metabolism of BVT.2938 was CYP1A1. CYP1A1 is regulated by the Ah receptor, is polymorphic and expressed predominantly in extrahepatic tissues including lungs, placenta, stomach and small intestine [19]. Since BVT.2938 was shown not to be involved in induction via the Ah receptor (data not shown), no risk for induction of the CYP1A1 was predicted. However, based on the results from these studies it might be anticipated that CYP1A1 might play a significant role in extra-hepatic clearance of BVT.2938 in the in vivo situation.

At least three of the metabolites of BVT.2938 were formed by CYP3A4, which is an abundant isoform of CYP in the liver known to be involved in the metabolism of many xenobiotics [20]. The main metabolite formed by CYP3A4 was M8, for which the K_m value was over 10 μM, and low intrinsic clearance. The results with ketoconazole, a specific inhibitor of CYP3A4 confirmed that this isoform was responsible for only approximately 20% of the total metabolism of the compound.

The experiments with liver slices showed also one additional important aspect of metabolism of BVT.2938, direct conjugation with sulfuric and glucuronic acid (via carbamate). Previous studies identified the metabolites [10], but no suitable model was found for kinetic studies of these reactions. These metabolites might represent an important pathway, especially in poor metabolizers of CYP2D6. This conclusion supports the previous suggestion, that several in vitro models should be used in parallel in order to discover all aspects of BVT.2938 metabolism [10].

In summary, in vitro metabolism of BVT.2938 was investigated in different in vitro models. The compound was shown to be a high clearance drug candidate with potential risk for metabolic drug interactions involving CYPs: 1A1 and 2D6*1. The major metabolite of BVT.2938 was formed by hydroxylation of the pyridine ring and this reaction was catalysed by CYP2D6*1. However, CYP1A1 was also involved in this reaction and its role in extra-hepatic metabolism of BVT.2938 might be significant. For a more complete understanding of the influence of polymorphic CYP2D6 and CYP1A1 on metabolism of BVT.2938 within population further studies using human hepatocytes and/or liver slices from extensive and poor metabolizers are recommended.

Acknowledgments

The authors thank Dr. Kathrin Sundberg and Dr. Ulf Martens for help with preparation and incubation of rat liver slices and Dr. Per Garberg for stimulating discussions.

References

[1] A.H. Mokdad, E.S. Ford, B.A. Bowman, W.H. Dietz, F. Vinicor, V.S. Bales, J.S. Markes, JAMA 289 (2003) 76–79.
[2] M. Ingelman-Sundberg, Toxicology 181–182 (2002) 447–452.
[3] W.E. Evans, H.L. McLeod, N. Engl. J. Med. 348 (2003) 538–548.
[4] T.D. Bjornsson, J.T. Callaghan, H.J. Einolf, V. Fischer, L. Gan, S. Grimm, J. Kao, P. King, G. Miwa, L. Ni, G. Kumar, J. McLeod, R.S. Obach, S. Roberts, M. Roe, A. Shah, F. Snikeris, J.T. Sullivan, D. Tweedie, J.M. Vega, J. Walsh, S.A. Wrighton, Drug Metab. Dispos. 31 (2003) 815–832.
[5] A. Mahgoub, J.R. Idle, L.G. Dring, R. Lancaster, R.L. Smith, Lancet 2 (1977) 584–586.
[6] W.E. Evans, M.V. Relling, Science 286 (1999) 487–491.
[7] G.T. Tucker, J.B. Houston, S.M. Huang, Pharm. Res. 18 (2001) 1071–1080.
[8] J.B. Houston, K.E. Kenworthy, A. Galetin, in: J.S. Lee, R.S. Obach, M.B. Fisher (Eds.), Drug Metabolising Enzymes. Cytochrome P450 and Other Enzymes in Drug Discovery and Development, Marcel Dekker Inc., New York, USA, 2003, pp. 211–254.
[9] R.S. Obach, A.E. Reed-Hagen, Drug Metab. Dispos. 30 (2002) 831–837.
[10] P.O. Edlund, P. Baranczewski, J. Pharm. Biomed. Anal. 34 (2004) 1079–1090.
[11] J.B. Houston, Biochem. Pharmacol. 47 (1994) 1469–1479.
[12] J.S. Lee, R.S. Obach, M.B. Fisher, Drug Metabolising Enzymes. Cytochrome P450 and Other Enzymes in Drug Discovery and Development, Marcel Dekker Inc., New York, USA, 2003.
[13] A. Asberg, Drugs 63 (2003) 367–378.
[14] T. Gura, Science 299 (2003) 849–852.
[15] S.G. Al-Dabbagh, J.R. Idle, R.L. Smith, J. Pharm. Pharmacol. 33 (1981) 161–164.
[16] S. Kobayashi, S. Murray, D. Watson, D. Sesardic, D.S. Davies, A.R. Boobis, Biochem. Pharmacol. 38 (1989) 2795–2799.
[17] H.M. Barham, M.S. Lennard, G.T. Tucker, Biochem. Pharmacol. 47 (1994) 1295–1307.
[18] T. Hiroi, T. Chow, S. Imaoka, Y. Funae, Drug Metab. Dispos. 30 (2002) 970–976.
[19] X. Ding, L.S. Kaminsky, Annu. Rev. Pharmacol. Toxicol. 43 (2003) 149–173.
[20] F.P. Guengerich, Annu. Rev. Pharmacol. Toxicol. 39 (1999) 1–17.